




Frequency analysis of extreme scour depths at bridge piers and their contribution to bridge collapse risk

Cristian Rifo, Pedro Arriagada, Bernd Ettmer & Oscar Link


To cite this article: Cristian Rifo, Pedro Arriagada, Bernd Ettmer & Oscar Link (2022) Frequency analysis of extreme scour depths at bridge piers and their contribution to bridge collapse risk, Hydrological Sciences Journal, 67:13, 2029-2041, DOI: [10.1080/02626667.2022.2122718](https://doi.org/10.1080/02626667.2022.2122718)

To link to this article: <https://doi.org/10.1080/02626667.2022.2122718>

 View supplementary material [↗](#)

 Published online: 17 Oct 2022.

 Submit your article to this journal [↗](#)

 Article views: 251

 View related articles [↗](#)

 View Crossmark data [↗](#)



Frequency analysis of extreme scour depths at bridge piers and their contribution to bridge collapse risk

Cristian Rifo^a, Pedro Arriagada^b, Bernd Ettmer^c and Oscar Link^a

^aDepartment of Civil Engineering, Faculty of Engineering, Universidad de Concepción, Concepción, Chile; ^bDepartment of Environmental Engineering, Faculty of Environmental Sciences, Universidad de Concepción, Concepción, Chile; ^cDepartment of Water, Environment, Construction and Safety, University of Applied Sciences Magdeburg-Stendal, Magdeburg, Germany

ABSTRACT

Bridge failures due to scour occur more frequently than expected, although bridge design considers conservative scenarios, evidencing a stochastic scour behaviour and the need for improvements in current design procedures. In this paper, a new method for determination of design local scour depth at bridge piers is proposed. The results show that peaks-over-threshold series are better suited than annual-maximum series of maximum scour depths for frequency analysis. Extreme scour depths follow the heavy-tailed Cauchy distribution. Scour depths with a 100-year return period resulted in 22 to 202% of the equilibrium scour depth currently used in design, evidencing the need for a different criterion to select the design scour depth. The proposed method computes the design local scour depth based on its probability of occurrence, introducing a novel probabilistic approach in bridge design for enhanced infrastructure risk management compatible with multi-hazard analysis.

ARTICLE HISTORY

Received 5 January 2022
Accepted 5 August 2022

EDITOR

A. Castellarin

ASSOCIATE EDITOR

A. Domeneghetti

KEYWORDS

extreme pier scour depths;
floods; Cauchy distribution;
risk management

1 Introduction

Local scour at bridge piers is an unsteady process controlled by non-linear relationships between the fluid, the flow, the pier, and the river sediments (Breusers *et al.* 1977, Raudkivi 1986, Dargahi 1990). In particular, the complex interplay between scouring and sediment deposition produces a high variation over time of the scour depth and bed level at piers (Lu *et al.* 2008, Hong *et al.* 2016, Link *et al.* 2020, Pizarro *et al.* 2020, Lee *et al.* 2021). The scour depth controls the hydraulic design of a bridge, and thus the estimation of its extreme maximum values is crucial for bridge safety. In practice, design schemes are based on enveloping curves, where design scour depth is considered the maximum scour depth caused by an extreme flood discharge, typically a discharge associated with a return period of 100 or 200 years, which is assumed to act on the streambed for the time period needed to achieve equilibrium scour. Such design approaches were adopted by, for example, Melville and Coleman (2000), MOP (2000), Arneson *et al.* (2012), and DWA (2020), and lead to good safety conditions (see e.g. Shahriar *et al.* 2021), even though scour-induced bridge failures occur more frequently than expected, under considerably scattered flood peak events (Wardhana and Hadipriono 2003, Cook *et al.* 2015, Tubaldi *et al.* 2017, Manfreda *et al.* 2018), evidencing a stochastic behaviour of scouring and the need for a different design approach.

Briaud *et al.* (2007) applied the SRICOS-EFA method of Briaud *et al.* (2004) to predict the scour depth versus time over the period of interest. As the SRICOS-EFA method does not consider sediment deposition, scour increased continuously until the end of the specified period, which is unrealistic in many cases such as during the falling limb of flood hydrographs.

Hydrological uncertainty was introduced in computing final scour depth for thousands of equally likely hydrographs, and the probability that a chosen scour depth will be exceeded was obtained from the final scour depth distribution. Manfreda *et al.* (2018) derived a probability distribution of scour depth, using simplified hydrographs of rectangular shape that produced a work on the scoured streambed equivalent to that produced by more realistic hydrographs. Scour depth was computed using the bridge-pier scour entropic (BRISSENT) model by Pizarro *et al.* (2017), which – like the SRICOS-EFA method (Briaud *et al.* 2004, 2007) – does not consider sediment deposition, thus leading to unrealistic time histories of scour in cases where refilling of the scour hole occurs.

Recent advances in scour research allow a precise computation of the time-dependent scour depth during floods (Borghei *et al.* 2012, López *et al.* 2014, Link *et al.* 2017) and the effects of sediment deposition on scour, especially during the falling limb of floods (Link *et al.* 2020, Flores-Vidriales *et al.* 2022), opening the possibility of a physically based approach for accurate computation of time-dependent scour depth.

Important research questions need to be answered for a probabilistic approach to estimate design scour depth. For example: Are annual maximum or partial duration series of extreme local scour depths better suited for frequency analysis of local scour? How are extreme scour depths distributed? What is the return period of equilibrium scour depth currently used in bridge design? What is the risk of bridge failure due to exceedance of a given design scour depth? A probabilistic approach for estimation of design scour depth would allow

more accurate bridge design and maintenance, increasing bridges' safety during their service life.

In this work, time series of scour at bridge piers are computed considering time-dependent local scour and sediment deposition. A frequency analysis of maximum scour depths considering peaks-over-threshold series (POT) and annual-maximum (AMAX) series is performed to obtain the probability density function of maximum scour depth. The design scour depth is determined from a frequency analysis for a given return period corresponding to an associated risk of bridge failure. The proposed new design philosophy is discussed in the contexts of improvement of bridge safety, bridge monitoring and maintenance.

The rest of this paper is organized as follows. Section 2 presents materials and methods including the study bridges, the generation of time-dependent scour depth, the selection of extreme value series and the best-fitting probability density function (PDF), as well as the computation of return period and risk of bridge failure. Section 3 presents an analysis of the obtained results, and section 4 presents a discussion of the proposed new design philosophy and

recommendations to improve bridge design, monitoring and maintenance.

2 Materials and methods

2.1 Study bridges

Ten bridges located in Chile, between latitudes $36^{\circ}32'$ and $40^{\circ}45'S$ and longitudes $72^{\circ}5'$ and $72^{\circ}58'W$, were considered in the present study, to cover a wide range of field conditions regarding flow, sediment and bridge pier geometry. Figure 1 shows the locations of the study bridges. Table 1 presents the main properties of the study bridges.

Sediment gradation curves were obtained from samples taken at each bridge site according to American Society for Testing and Materials (ASTM) sampling standards (ASTM 2017, 2018, 2019). Figure 2 shows the sieve curves for the riverbed sediments at the study bridges. A wide range of sediments were present at the different study bridges, varying from very fine sand to cobbles.

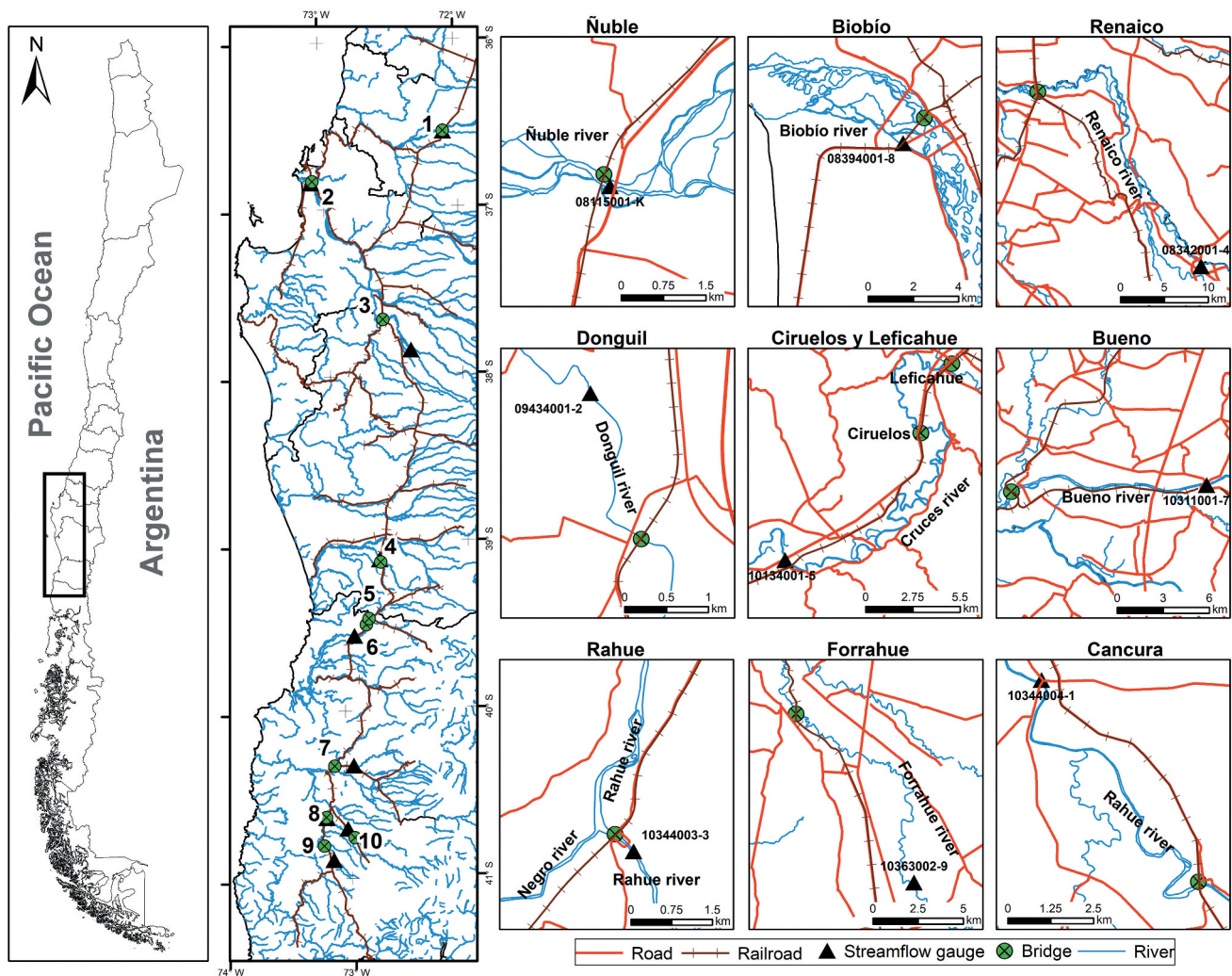
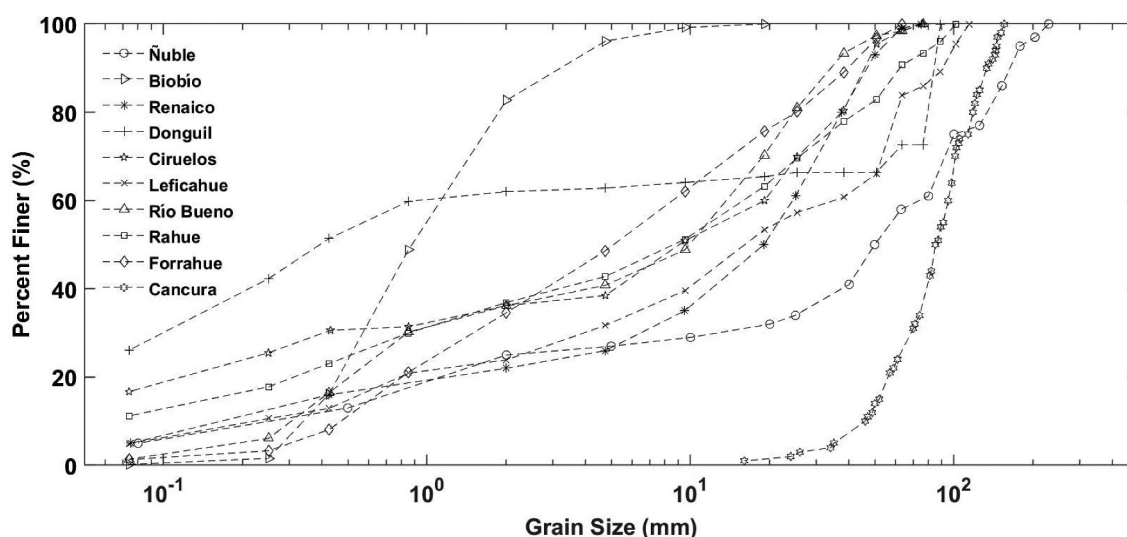


Figure 1. Locations of the study bridges.

Table 1. Main properties of the study bridges.

No.	Bridge	Lat.	Long.	Type	Age	Pier diameter (m)	Watershed area (km ²)	Pier shape
1	Ñuble	36°32'S	72°5'W	Railway	97	2.5	2973	Cylindrical
2	Biobío	36°49'S	73°5'W	Railway	130	0.4	21217	Cylindrical
3	Renaico	37°40'S	72°35'W	Railway	88	4.1	1493	Round nose
4	Donguil	39°7'S	72°40'W	Railway	115	2.8	739	Cylindrical
5	Ciruelos	39°29'S	72°48'W	Railway	111	2.7	1635	Cylindrical
6	Leficahue	39°27'S	72°47'W	Railway	111	2.5	648	Cylindrical
7	Bueno	40°19'S	73°6'W	Railway	138	2.5	4483	Cylindrical
8	Rahue	40°37'S	73°10'W	Railway	114	2.5	2124	Cylindrical
9	Forrahue	40°48'S	73°12'W	Railway	111	4.2	200	Rectangular
10	Cancura	40°45'S	72°58'W	Highway	43	2.0	1837	Complex

**Figure 2.** Sieve curves of the riverbed sediments at the study bridges.**Table 2.** Streamflow gauges (SFG).

ID	Bridge	SFG code	Lat. (S)	Long. (W)	Record period	Altitude (m.a.s.l.)
1	Ñuble	8115 001-K	36°33'00"	72°05'60"	1956–1982	107
2	Biobío	8394 001-8	36°50'16"	73°03'41"	1970–2020	16
3	Renaico	8342 001-4	37°50'41"	72°23'27"	1982–2019	135
4	Donguil	9434 001-2	39°07'03"	72°40'44"	1947–2019	85
5	Ciruelos	10134 001-5	39°33'12"	72°54'02"	1969–2020	60
6	Leficahue	10134 001-5	39°33'12"	72°54'02"	1969–2020	60
7	Bueno	10311 001-7	40°19'43"	72°57'27"	1926–2019	45
8	Rahue	10344 003-3	40°38'00"	73°10'53"	2008–2020	40
9	Forrahue	10344 004-1	40°42'21"	73°01'08"	2008–2020	50
10	Cancura	10363 002-9	40°54'16"	73°07'54"	1991–2019	117

2.2 Streamflow data

Time series of streamflow were obtained from gauges (streamflow gauges, SFGs) close to the study bridges. SFGs are administered by the National Water Agency (DGA 2021). Table 2 presents the available SFG for each bridge. Figure 3 shows the daily records for each SFG. Flow series present different record periods and numerous information gaps of various length. To fill the gaps in the daily mean discharge series a number of techniques are available, which vary from simple interpolation to models and complex statistical analysis (Gyau-Boakye and Schultz 1994). Harvey *et al.* (2012) distinguished six classes of methods according to their mathematical complexity, namely manual inference, serial interpolation techniques, scaling factors, equipercntile techniques, linear regression, and

hydrological modelling. Further, a number of machine learning methods have been applied to infill missing flow data, including artificial neuronal networks (e.g. Mwale *et al.* 2012, Kim *et al.* 2015, Ben Aissia *et al.* 2017, Vega-García *et al.* 2019), random forest models (Breiman 2001, Stekhoven and Bühlmann 2012) and stochastic non-parametric methods such as direct sampling (Dembélé *et al.* 2019). Advantages of missForest models over other alternatives for infilling daily streamflow data are: (1) they can quickly handle large amounts of data and the missing data imputation is unsupervised and automatic, avoiding the determination of predictor stations (Sidibe *et al.* 2018); (2) they can handle multiple data gaps in the series (Tang and Ishwaran 2017); (3) they are easy to implement in computational languages such as R, as they do not require initial setting and

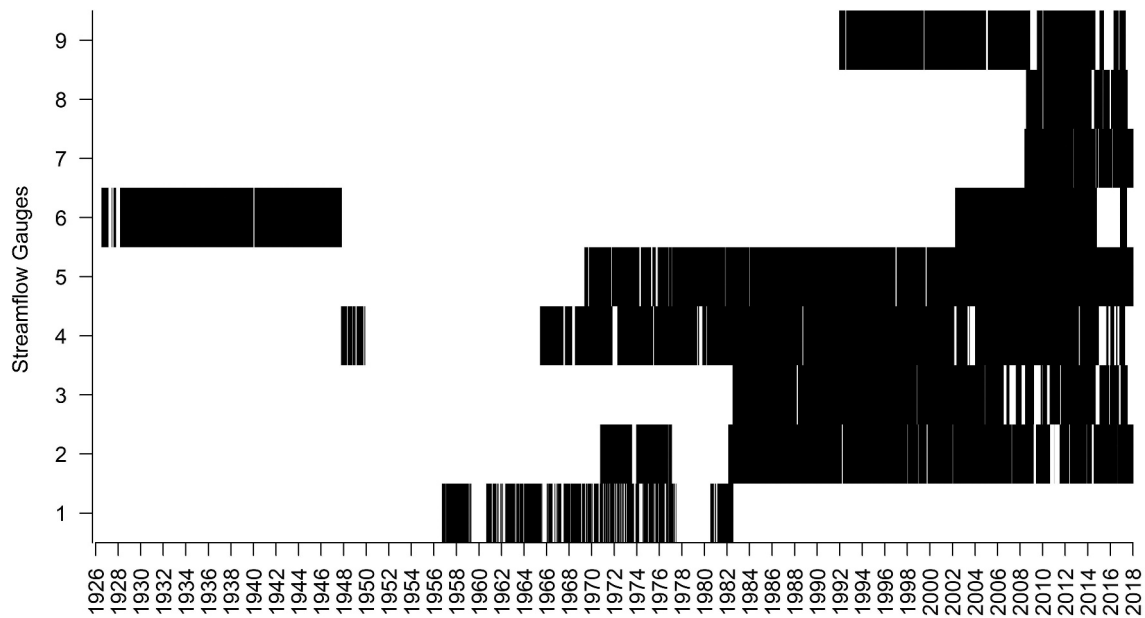


Figure 3. Available and missing data in the data records from the nine streamflow gauges.

calibration of parameters (Muñoz *et al.* 2018); and (4) they achieve competitive predictive performance and are computationally efficient, making them suitable for real-world prediction tasks (Sidibe *et al.* 2018). Arriagada *et al.* (2021) showed that missForest allows a precise and reliable simulation of the missing data quickly and automatically. Thus, complete series of daily mean flows were generated for the period 1970 to 2016 applying the missForest machine learning algorithm as proposed by Arriagada *et al.* (2021).

2.3 Flow velocity and flow depth computation

Rating curves relating the flow velocity and depth with the river discharge as well as the relationship of the Froude and densimetric Froude numbers with the discharge were computed with the one-dimensional hydraulic model Hydrologic Engineering Center's River Analysis System (HEC-RAS) 5.0.7. For the simulations, digital elevation models were obtained from topographic and bathymetric surveys conducted by Empresa de Ferrocarriles del Estado (EFE) (2020). The Manning roughness coefficient was estimated using the Strickler equation and Cowan method described in Chow (1994). Flow properties were evaluated for discharges covering the range of the hydrograph for the study period at each site. Figure 4 shows the digital elevation models with estimated Manning's roughness coefficient, the bridge section view, and obtained curves of flow velocity, depth, Froude number and densimetric Froude number over the discharge for the study bridges.

2.4 Time-dependent scour and deposition at bridge piers

The time-dependent local scour depth at bridge piers was computed with the dimensionless effective flow work (DFW) model, by Pizarro *et al.* (2017) and Link *et al.* (2020). The mathematical definition of the dimensionless effective flow work W^* is:

$$W^* = \int_0^{t_{end}} \frac{Fr_d^3 u_{ef}}{z_R} \delta dt (1)$$

where $Fr_d = u_{ef}/\sqrt{\rho'gd_s}$ is the densimetric Froude number, $u_{ef} = u - u_{cs}$ is the excess velocity above the incipient scour condition $u_{cs}(=0.5u_c)$, u is the average flow velocity, u_c is the critical velocity for the inception of sediment motion at the undisturbed bed, $z_R = D^2/2d_s$ is a reference length, D is the pier diameter, d_s is the representative sediment particle diameter (e.g. d_{50}), t_{end} is a considered time for analysis purposes (e.g. hydrograph duration for event-scale analysis), and δ is the delta Dirac function,

$$\delta = \begin{cases} 0 & u/u_{cs} < 1.0 \\ 1 & u/u_{cs} \geq 1.0 \end{cases} (2)$$

The DFW model uses a three-parameter exponential relationship between W^* and the normalized scour depth $Z^*(=z_s/z_R)$ which is reported in Equation (3):

$$Z^* = c_1(1 - \exp(-c_2 W^{c_3})), (3)$$

where z_s is the dimensional scour depth, whereas c_1 , c_2 , and c_3 are model coefficients. It is worth noting that c_1 corresponds to the dimensionless equilibrium scour depth:

$$c_1 = Z_{eq}^* = z_{eq} \left(\frac{2d_s}{D^2} \right), (4)$$

The equilibrium scour depth, z_{eq} , was computed with the scour equation of Sheppard *et al.* (2014):

$$\frac{z_{eq}}{a^*} = 2.5f_1f_2f_3, \quad 0.4 \leq \frac{u}{u_c} < 1.0 (5)$$

$$f_1 = \tanh \left[\left(\frac{h}{a^*} \right)^{0.4} \right], (6)$$

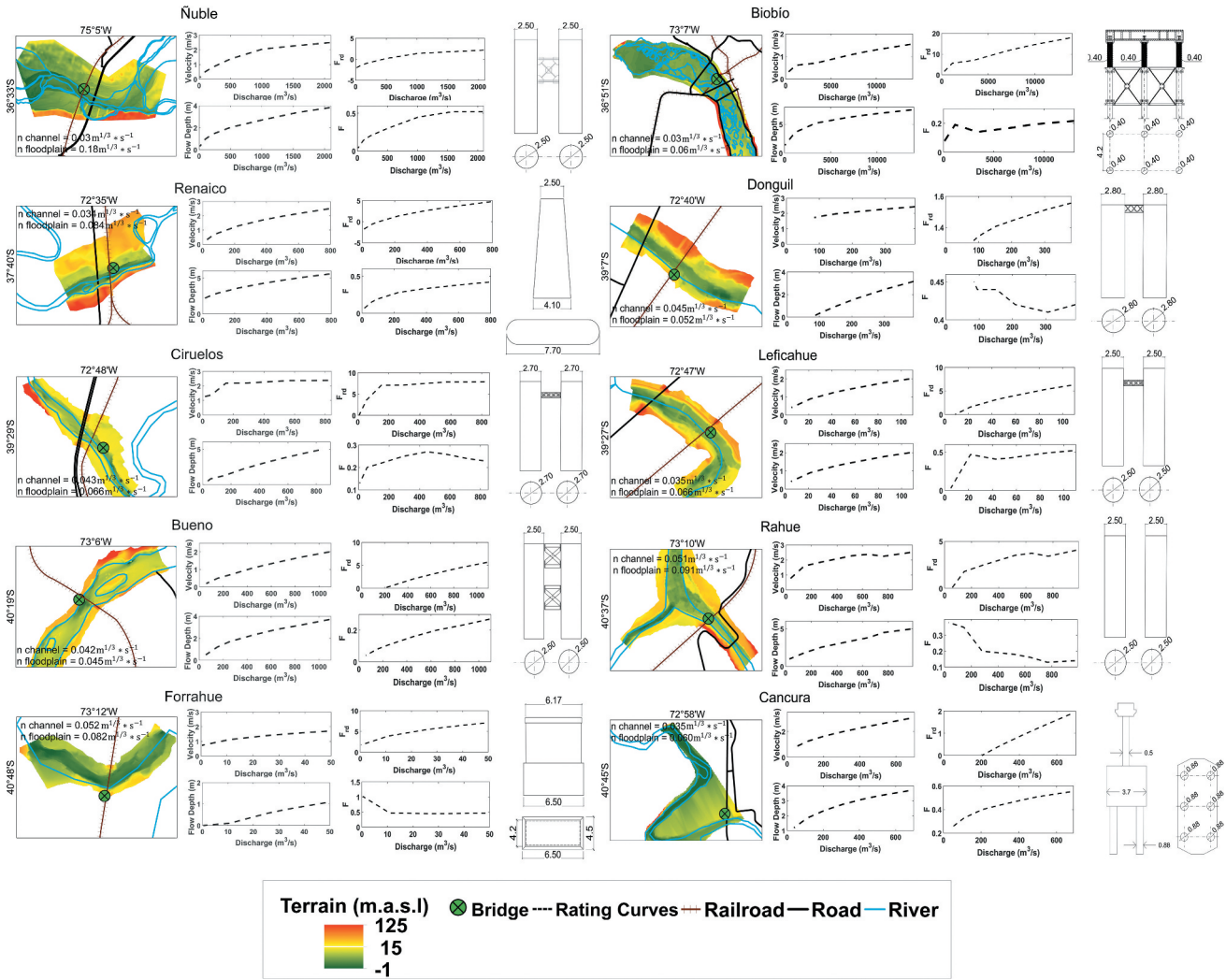


Figure 4. Digital elevation models with Manning's roughness coefficient, side view of bridges, rating curves and relations between Froude and densimetric Froude over discharge for the study bridges.

$$f_2 = \left\{ 1 - 1.2 \left[\ln \left(\frac{u}{u_c} \right) \right]^2 \right\}, \quad (7)$$

$$f_3 = \left[\frac{\left(\frac{a^*}{d_s} \right)}{0.4 \left(\frac{a^*}{d_s} \right)^{1.2} + 10.6 \left(\frac{a^*}{d_s} \right)^{-0.13}} \right], \quad (8)$$

where Z_{eq}^* is the dimensionless equilibrium scour depth, z_{eq} is the dimensional equilibrium scour depth, $a^* (= K_s a_p)$ is the effective diameter of the pier, K_s is the shape factor, a_p is the projected width of the pier, and h is the flow depth. Besides, u_c was computed following Zanke's equation (Zanke 1977):

$$u_c = 1.4 \left(\sqrt{\rho' g d_s} + 10.5 v / d_s \right). \quad (9)$$

On the other side, c_2 and c_3 can take values according to geometrical, flow, and sediment properties. Sediment deposition refers herein to the process of refilling the scour hole. Deposition occurs when the sediment supply rate of sediment particles into the scour hole is greater than the local sediment transport capacity:

$$z_d[i] = \begin{cases} 0, & \xi g_s^* [i-1,j] \leq g_s^* [i,j] \\ \frac{\alpha}{\rho_s (1-p)} \sum_{j=1}^n \left(\frac{\xi g_s^* [i-1,j] - g_s^* [i,j]}{z_{i-1}} \right) \Delta t, & \xi g_s^* [i-1,j] > g_s^* [i,j] \end{cases} \quad (10)$$

where $z_d[i]$ is the sediment deposition depth, j is a counter for the considered sediment sizes in the sieve curve and i reports the discrete-time instant, p is the riverbed porosity, g_s^* is the sediment transport capacity, ξg_s^* is the sediment supply rate, and α and ξ are calibration parameters. It is worth noting that ξ is an exceedance sediment supply coefficient, whereas the final scour depth – considering both the erosive and refilling processes – at each temporal instant i , was computed as $z_{[i]} = z_{s[i]} - z_d[i]$ and $W_{[i]}^* = W_{s[i]}^* - \Delta W_{d[i]}^*$ (note that the subscripts “s” and “d” are used for scour and deposition, respectively). Finally, g_s^* was estimated using the Meyer-Peter and Müller equation (Meyer-Peter and Müller 1948):

$$g_s^* = 8 \rho_s (\rho' g d_s^3)^{0.5} \left[\left(\frac{C_R}{C'_R} \right)^{1.5} \Theta - \Theta_c \right]^{1.5} \quad (11)$$

where C_R is the total Chézy coefficient due to effective bed roughness k_s ($= 18 \log(12h/k_s)$), C'_R is the Chézy coefficient

Table 3. Parameters of the DFW model for the study bridges.

	ξ	α	c_1	c_2	c_3	$D_{50}(mm)$	$D_{90}(mm)$	$D(m)$	S
Ñuble	4.0	0.00020	0.0800	0.031	0.23	50.0	163.6	2.5	0.0020
Biobío	2.5	0.00020	0.0100	0.010	0.37	0.92	3.200	0.3	0.0002
Renaico	2.5	0.00020	0.0120	0.040	0.27	20.0	47.49	4.1	0.0029
Donguil	2.5	0.00200	0.0003	0.010	0.30	0.40	84.26	2.5	0.0010
Ciruelos	2.5	0.02250	0.0250	0.028	0.25	8.69	45.86	2.7	0.0020
Leficahue	2.5	0.00020	0.0060	0.028	0.30	8.84	62.36	2.5	0.0025
Bueno	2.5	0.00002	0.0150	0.030	0.30	10.1	34.60	2.5	0.0070
Rahue	2.5	0.00020	0.0350	0.031	0.23	24.8	81.95	2.5	0.0010
Forrahue	2.5	0.00225	0.0015	0.028	0.28	5.25	39.75	4.2	0.0060
Cancura	5.0	$1 * 10^{-9}$	0.1800	0.010	0.20	85.0	133.0	2.0	0.0740

due to particle roughness d_{90} ($= 18\log(12h/d_{90})$), and Θ and Θ_c are the Shields and threshold Shields parameters. Table 3 shows the parameters for computation of time-dependent pier scour depth with the DFW model at the study bridges. Model formulation considers the possibility that deposition is higher than scour, producing negative values of the bed level, which corresponds well with the physics. However, to be conservative in the analysis of extreme scour values we limited the minimum value of the bed level to zero, as values over the original bed level might involve other complex sediment transport processes such as migrating bedforms that are not represented in the model. However, the effect of this limitation on the extreme scour depths series is small.

2.5 Extreme scour depth series

A main issue to be tackled for the frequency analysis of extreme maximum scour depths is the selection of values used to build the time series of extreme values. Following Cunnane (1973), two time series commonly used in flood frequency analysis were evaluated, namely POT and AMAX. For a POT series a threshold value was established for the choice of the magnitudes of the local scour (a value per year that exceeds the limit value) following the methodology proposed by Lang *et al.* (1999). As a general rule, a minimum of 30 data points were established on the threshold value for the frequency analysis of the local scour, as scour at piers varies with streamflow and thus it is practical to adopt the same record length for frequency analysis of both extreme values, floods and scour. In this regard, several studies analysed the effect of record length on the accuracy of frequency analysis results (Kobierska *et al.* 2017, Yan *et al.* 2021). For example,

Stedinger *et al.* (1993) recommended a record length of 30 years for flood frequency analysis. Similarly, Li *et al.* (2018) showed that a 30-year hydrological sample size in water resources management is sufficient for hydrological design. The best series for frequency analysis was selected according to the efficiency:

$$E = \frac{\text{var}(Z_s(T)_{AMAX})}{\text{var}(Z_s(T)_{POT})} \quad (12)$$

where E is efficiency, *var* is the variance, and $Z_s(T)$ is the local scour depth corresponding to a return period of T years. Efficiencies where $E > 1$ suggest the POT series is better, $E < 1$ suggest the AMAX series is better, and $E = 1$ suggest that both series are equally good for frequency analysis.

2.6 Distribution of extreme local scour depths

The maximum likelihood method was applied to fit probability distributions representing the series of extreme maximum scour depths. Table 4 shows the cumulative probability distribution functions for analysis.

The goodness of fit was determined for each probability distribution using the Kolmogorov-Smirnov (KS), χ^2 , and Anderson-Darling (AD) tests with a significance level of 0.05, and the coefficient of determination (r^2), the Akaike information criterion (AIC), and the minimum value of Bayesian information criterion (BIC), as shown in Table 5, where n is the sample size, $F(x)$ is the theoretical cumulative distribution function, $F_n(x)$ is the empirical cumulative distribution function, k is the class intervals, O_i is the observed absolute frequency and E_i is the theoretical frequency in interval i , \sup is the largest absolute difference, \hat{y}_i is the fitted value, \bar{y} is the mean, y_i is the observed

Table 4. Cumulative distribution functions used in this study.

Distribution	Cumulative distribution function	Parameter
Normal	$F(x) = (\sqrt{2\pi})^{-1} \int_0^x e^{-t^2/2} dt \left(\frac{x-\mu}{\sigma}\right)$	μ : Location parameter σ : Scale parameter
Lognormal	$F(x) = (\sqrt{2\pi})^{-1} \int_0^x e^{-t^2/2} dt \left(\frac{\ln(x-\mu)}{\sigma}\right)$	y : Location parameter μ : Scale parameter σ : Shape parameter
Weibull	$F(x) = 1 - \exp\left[-\left(\frac{x-y}{\beta}\right)^\alpha\right]$	y : Location parameter β : Scale parameter α : Shape parameter
Gamma	$F(x) = \frac{\Gamma((x-y)/\beta)^\alpha}{\Gamma(\alpha)}$ Γ_z : Incomplete gamma function	y : Location parameter β : Scale parameter α : Shape parameter
Gumbel	$F(x) = \frac{1}{\beta} \exp\left[-\frac{x-\mu}{\beta} - e^{-\frac{x-\mu}{\beta}}\right]$	μ : Location parameter β : Scale parameter
Cauchy	$F(x) = \frac{1}{2} + \frac{1}{\pi} \tan^{-1}\left(\frac{x-\mu}{\sigma}\right)$	μ : Location parameter σ : Scale parameter

Table 5. Goodness of fit statistics.

Statistics	General equation
r^2	$\frac{\sum_{i=1}^n (y_i - \bar{y})^2}{\sum_{i=1}^n (y_i - \bar{y})^2}$
KS	$\sup F_n(x) - F(x) $
χ^2	$\sum_{i=1}^k \frac{(O_i - E_i)^2}{E_i}$
AD	$n \int_{-\infty}^{\infty} \frac{[F_n(x) - F(x)]^2}{F(x)[1 - F(x)]} dF(x)$
AIC	$-2\ell(\hat{\theta}_{n,k}) + 2k$
BIC	$-2\ell_{n,i}(\hat{\theta}_n^i) + 2k_i \log(n)$

values of the dependent variable, $\ell(\hat{\theta}_{n,k})$ is the log-likelihood of θ and $\ell_{n,i}(\hat{\theta}_n^i)$ is the log-likelihood corresponding to the model. Additionally, a graphic analysis of the data series and fitting curves was performed to complement the information gained from the goodness-of-fit test and criteria.

2.7 Return period of equilibrium scour depth

The return period of a given scour depth was determined from the selected probability distribution function, as the inverse of the exceedance probability.

2.8 Contribution of local scour to bridge collapse risk

The contribution of local scour to bridge collapse risk was computed through the hydrological risk R that a flood with a return period equal to T is exceeded during the design life, L_t , of the bridge:

$$R = 1 - (1 - 1/T)^{L_t} \tag{13}$$

In the present study, a service life of 60 years was adopted for the study bridges.

3 Results

3.1 Time-dependent local scour depth at bridge piers

Figure 5 shows the computed time-dependent local scour depth for the study bridges according to parameters in Table 3.

The resulting scour is highly dynamic in time, with important variations during the study period (1970–2016). Seven out of 10 cases (a, b, c, e, g, i, and j) presented sediment deposition that was able to reverse scour to zero several times, while cases d, f, and h presented scour depth higher than zero during the whole period. In all cases, the number of local maxima was higher than the number of years under analysis. It is worth noting that some sites exhibited similar scour maxima (e.g. cases a, e, h, and j) while others exhibited maxima with notably different magnitudes (e.g. cases b and g).

3.2 Extreme scour depths series

Table 6 shows the efficiency for selection of series of extreme maximum scour depths at study bridges for different return periods.

In terms of efficiency, $E > 1$ in 24 of 40 cases; $E = 1$ in seven cases, and $E < 1$ in nine cases. Consequently, the POT series were in general equal to or better (24 + 7 = 31 out 40) than the AMAX series for frequency analysis of maximum local scour depths, and are thus selected for the frequency analysis.

3.3 Extreme local scour depth distribution

Table 7 shows the goodness-of-fit statistics and fit criteria of the distributions fitted to the POT series for the study bridges. Graphs with the probability density, histogram, cumulative distribution, and P-P plots are included in the Supplementary material.

All candidate PDFs presented acceptable goodness-of-fit statistics. According to the statistical tests and criteria, there is no single PDF that performs best in all study bridges. Thus, the sensitivity of the extreme values to the return period was analysed as an additional criterion for PDF selection. Table 8 shows the local scour depth computed with the different distributions. Scour depths computed with Weibull, normal, log-normal, gamma and Gumbel distributions presented very low or no sensitivity to the return period, which is not realistic. In contrast, the Cauchy distribution computed realistic variations of scour magnitudes with the return period. Thus, it was selected as the best distribution representing extreme local scour depths at bridges.

3.4 Return period of equilibrium scour depth

Table 9 shows the equilibrium scour and corresponding return period computed from the Cauchy probability distribution function. The return period of the equilibrium local scour was more than 100 years in six out of 10 study bridges, and less than 100 years in four of the study bridges. It presented important variability among the study bridges, ranging between 25 and 570 years, which evidences the lack of a consistent criterion for the determination of design scour depth in current design methods. Conversely, scour depth with a 100-year return period resulted in 22 to 202% of the equilibrium scour depth currently used in design.

3.5 Return period and risk of bridge failure due to exceedance of design local scour depth

Table 10 shows the computed local scour depth for different return periods and risk levels at the study bridges. The magnitude of local scour depth at bridge piers corresponding to a given return period present a great variation among the study sites.

4 Discussion

Current standards in hydraulic bridge design consider a design scour depth that corresponds to the equilibrium scour. In practice, equilibrium scour is computed for the worst-case scenario given by an extreme flood, assuming that its duration is longer than that needed to develop and achieve equilibrium scour. An important shortcoming of this design approach is that magnitudes of resulting design scour are not associated to an exceedance probability or

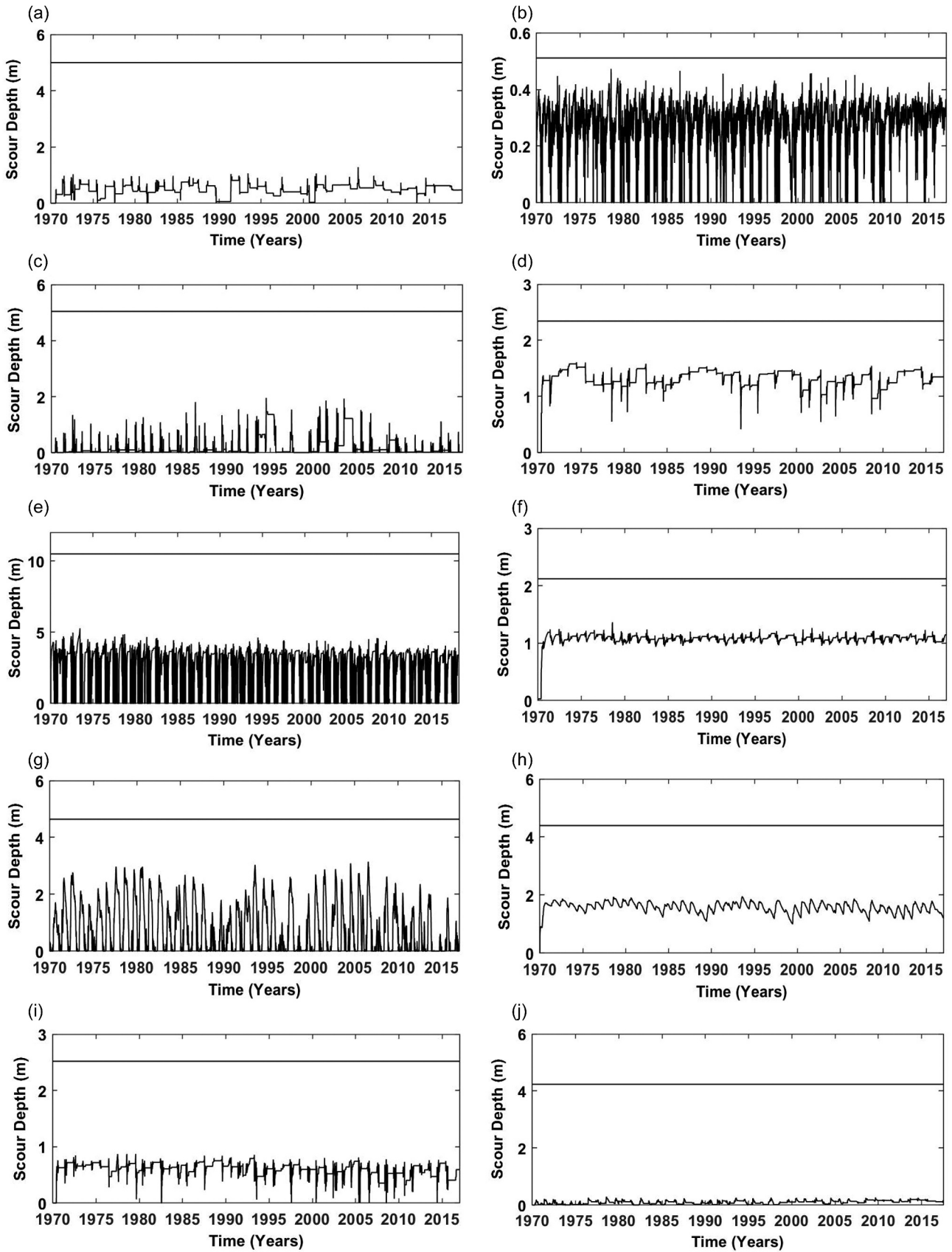


Figure 5. Computed time-dependent local scour depth at bridges (a) Nuble, (b) Biobío, (c) Renaico, (d) Donguil, (e) Ciruelos, (f) Leficahue, (g) Bueno, (h) Rahue, (i) Forrahue, and (j) Cancura. The solid line is the equilibrium scour depth corresponding to c_1 .

Table 6. Efficiency for selection of series of extreme maximum scour depths.

T	Ñuble	Biobío	Renaico	Donguil	Ciruelos	Leficahue	Bueno	Rahue	Forrahue	Cancura
25	1.19	1.22	0.94	1.0	0.73	1.04	0.91	1.00	1.16	1.22
50	1.22	1.22	0.94	1.0	0.74	1.04	1.00	1.01	1.16	1.23
100	1.26	1.22	0.93	1.0	0.75	1.04	1.00	1.02	1.16	1.24
200	1.29	1.22	0.93	1.0	0.76	1.03	1.03	1.03	1.17	1.25

Table 7. Goodness-of-fit statistics of the distributions fitted to the POT series for the study bridges.

Bridge	Distribution	Goodness-of-fit statistic			Goodness-of-fit criteria		
		KS	χ^2	AD	AIC	BIC	r^2
Ñuble	Cauchy	0.15	1.61	1.17	-20.32	-17.21	0.66
	Weibull	0.11	0.83	0.57	-41.08	-37.97	0.95
	Normal	0.14	6.45	0.62	-41.69	-38.58	0.97
	Lognormal	0.16	3.82	0.66	-41.60	-38.49	0.96
	Gamma	0.16	5.44	0.64	-41.78	-38.67	0.97
Biobío	Gumbel	0.17	3.83	0.73	-40.10	-36.99	0.93
	Cauchy	0.19	3.91	1.99	-166.76	-163.48	0.67
	Weibull	0.17	2.89	1.73	-168.57	-165.29	0.83
	Normal	0.17	3.14	1.13	-178.50	-175.22	0.92
	Lognormal	0.16	3.36	1.01	-180.03	-176.76	0.94
Renaico	Gamma	0.16	3.19	1.05	-179.54	-176.27	0.93
	Gumbel	0.12	0.55	0.54	-186.56	-183.28	0.98
	Cauchy	0.16	1.1	1.08	61.62	64.94	0.64
	Weibull	0.13	3.66	0.57	39.69	43.01	0.97
	Normal	0.14	2.9	0.65	40.78	44.11	0.96
Donguil	Lognormal	0.13	4.41	0.75	38.58	41.91	0.97
	Gamma	0.14	5.32	0.66	38.40	41.73	0.97
	Gumbel	0.13	7.38	0.77	39.20	42.53	0.96
	Cauchy	0.16	1.72	1	-74.75	-71.75	0.71
	Weibull	0.14	1.84	1.01	-83.15	-80.15	0.88
Ciruelos	Normal	0.12	1.98	0.56	-90.08	-87.09	0.96
	Lognormal	0.12	2.3	0.51	-90.73	-87.74	0.96
	Gamma	0.12	2.06	0.53	-90.52	-87.53	0.96
	Gumbel	0.11	1.96	0.37	-93.39	-90.40	0.98
	Cauchy	0.14	0.19	0.55	-19.15	-15.58	0.8
Leficahue	Weibull	0.18	2.75	1.56	-43.94	-40.37	0.82
	Normal	0.14	1.09	0.58	-43.51	-39.94	0.91
	Lognormal	0.13	1.6	0.46	-42.81	-39.24	0.93
	Gamma	0.13	0.85	0.49	-43.09	-39.52	0.92
	Gumbel	0.09	0.04	0.23	-37.56	-33.99	0.97
Río Bueno	Cauchy	0.15	3.09	1.05	-119.86	-116.75	0.78
	Weibull	0.23	3.61	3.02	-101.60	-98.49	0.72
	Normal	0.14	1.86	1.05	-122.61	-119.50	0.82
	Lognormal	0.13	1.81	0.93	-124.58	-121.47	0.83
	Gamma	0.14	1.48	0.97	-123.94	-120.83	0.83
Rahue	Gumbel	0.12	0.43	0.43	-135.82	-132.71	0.91
	Cauchy	0.12	0.44	0.68	44.21	47.32	0.73
	Weibull	0.08	2.18	0.23	28.24	31.35	0.99
	Normal	0.1	2.61	0.34	29.41	32.52	0.98
	Lognormal	0.13	3.97	0.53	31.38	34.49	0.96
Forrahue	Gamma	0.12	4.06	0.45	30.55	33.66	0.97
	Gumbel	0.16	5.84	0.84	35.80	38.91	0.91
	Cauchy	0.12	6.61	1.1	-64.44	-60.97	0.79
	Weibull	0.09	0.84	0.47	-76.55	-73.08	0.97
	Normal	0.1	4.02	0.31	-80.50	-77.03	0.98
Cancura	Lognormal	0.11	5.15	0.36	-80.22	-76.74	0.98
	Gamma	0.1	3.46	0.34	-80.35	-76.88	0.98
	Gumbel	0.13	7.33	0.85	-74.32	-70.85	0.94
	Cauchy	0.19	1.95	1.65	-104.62	-101.68	0.65
	Weibull	0.19	2.81	1.87	-105.07	-102.13	0.81
Cancura	Normal	0.17	2.47	1.34	-113.15	-110.22	0.9
	Lognormal	0.17	2.62	1.22	-114.38	-111.45	0.91
	Gamma	0.17	2.52	1.26	-113.99	-111.06	0.91
	Gumbel	0.13	1.65	0.7	-120.56	-117.63	0.95
	Cauchy	0.17	3.34	1.47	-126.58	-123.47	0.67
Cancura	Weibull	0.14	4.35	0.96	-145.42	-142.30	0.9
	Normal	0.15	5.15	1.05	-148.33	-145.22	0.94
	Lognormal	0.14	5.66	1.06	-149.19	-146.08	0.94
	Gamma	0.15	5.35	1.06	-149.01	-145.90	0.94
	Gumbel	0.15	12.88	1.11	-149.21	-146.10	0.93

Table 8. Local scour depth for return periods of 25, 50, 100 and 200 years computed with the different distributions.

Bridge	Distribution	$Z_s(m)$			
		T = 25	T = 50	T = 100	T = 200
Ñuble	Cauchy	1.60	2.40	4.00	7.11
	Weibull	1.05	1.08	1.10	1.12
	Normal	1.07	1.11	1.14	1.17
	Lognormal	1.09	1.14	1.19	1.24
	Gamma	1.08	1.13	1.17	1.21
	Gumbel	1.15	1.22	1.30	1.38
Biobío	Cauchy	0.50	0.60	0.79	1.17
	Weibull	0.46	0.46	0.47	0.47
	Normal	0.46	0.46	0.47	0.47
	Lognormal	0.46	0.46	0.47	0.48
	Gamma	0.46	0.46	0.47	0.48
	Gumbel	0.46	0.47	0.48	0.49
Renaico	Cauchy	3.34	5.56	9.98	18.82
	Weibull	1.86	1.97	2.07	2.16
	Normal	1.85	1.96	2.07	2.17
	Lognormal	2.01	2.23	2.44	2.66
	Gamma	1.93	2.10	2.26	2.42
	Gumbel	2.02	2.25	2.48	2.70
Donguil	Cauchy	1.78	2.09	2.77	3.99
	Weibull	1.58	1.60	1.61	1.62
	Normal	1.58	1.60	1.62	1.63
	Lognormal	1.59	1.60	1.62	1.64
	Gamma	1.59	1.60	1.62	1.64
	Gumbel	1.61	1.64	1.67	1.70
Ciruelos	Cauchy	5.47	6.53	8.67	12.93
	Weibull	4.96	5.02	5.08	5.13
	Normal	4.90	4.98	5.05	5.12
	Lognormal	4.91	4.99	5.07	5.14
	Gamma	4.91	4.99	5.06	5.13
	Gumbel	4.96	5.10	5.23	5.37
Leficahue	Cauchy	1.36	1.53	1.86	2.53
	Weibull	1.29	1.30	1.31	1.32
	Normal	1.27	1.28	1.29	1.30
	Lognormal	1.27	1.28	1.30	1.31
	Gamma	1.27	1.28	1.30	1.31
	Gumbel	1.27	1.29	1.31	1.33
Río Bueno	Cauchy	4.28	5.98	9.37	16.14
	Weibull	3.09	3.16	3.22	3.27
	Normal	3.16	3.26	3.36	3.44
	Lognormal	3.23	3.37	3.51	3.63
	Gamma	3.20	3.33	3.45	3.56
	Gumbel	3.47	3.72	3.96	4.20
Rahue	Cauchy	1.99	2.42	3.30	5.01
	Weibull	1.69	1.71	1.72	1.74
	Normal	1.70	1.73	1.75	1.77
	Lognormal	1.71	1.74	1.76	1.79
	Gamma	1.70	1.73	1.76	1.78
	Gumbel	1.78	1.84	1.90	1.96
Forrahue	Cauchy	0.94	1.10	1.40	2.08
	Weibull	0.86	0.87	0.88	0.88
	Normal	0.86	0.87	0.88	0.89
	Lognormal	0.86	0.87	0.88	0.90
	Gamma	0.86	0.87	0.88	0.89
	Gumbel	0.86	0.88	0.90	0.92
Cancura	Cauchy	0.40	0.57	0.90	1.62
	Weibull	0.27	0.28	0.28	0.29
	Normal	0.27	0.28	0.29	0.29
	Lognormal	0.27	0.28	0.29	0.30
	Gamma	0.27	0.28	0.29	0.30
	Gumbel	0.28	0.30	0.32	0.33

to a return period. Consequently, risk of failure due to scour cannot be calculated. Probabilistic scour estimations through uncertainty analysis were proposed in the past (e.g. Johnson and Ayyub 1992, Johnson and Dock 1998, Bolduc *et al.* 2008). The developed probabilistic models for the final scour depth were used to assess the probability that a specified threshold depth is exceeded at a bridge pier for given hydrological variables considering model, hydraulic, and/or parameter uncertainties. In such

models huge uncertainties need to be assumed and applications to specific cases show that the results exaggerate the exceedance probabilities. For example, Khalid *et al.* (2019) and Contreras-Jara *et al.* (2021) obtained a probability of 0.5 for the occurrence of design scour under design conditions – or, in other words, after a design flood 50% of the bridges would exhibit design scour while 50% would not. Recognizing that uncertainty is inherent to scour modelling, it seems obvious that progress in scour research allows

Table 9. Return period of equilibrium scour depth of the distribution Cauchy.

Study site	Z_{eq} (m)	Z_{eq}^*	T (years)
Ñuble	5.0	0.0800	133
Biobío	0.5	0.0100	25
Renaico	5.0	0.0120	43
Donguil	2.3	0.0003	65
Ciruelos	10.5	0.0250	140
Leficahue	2.1	0.0060	133
Río Bueno	4.6	0.0150	30
Rahue	4.4	0.0350	168
Forrahue	2.5	0.0015	270
Cancura	4.2	0.1800	570

more certainty than flipping a coin. In this paper, a possible way forward based on frequency analysis of extreme values was proposed and shown to work well in 10 study bridges.

The obtained time-dependent scour (Fig. 5) was very sensitive to the involved case-specific model parameters (Table 3), presenting noticeable differences among the study bridges. The scour-deposition model adequately differentiated between the study cases and produced realistic scour. Alternative methods for the time-dependent scour, such as those by Zanke (1982) or Dey (1999), could also be applied. In the proposed method, constant c_1 was evaluated with the scour equation by Sheppard *et al.* (2014), which is conservative as it neglects the possible effects of armouring. Different scour equations could be used as an alternative to Sheppard *et al.* (2014) for estimation of c_1 , such as those proposed by Jain and Fischer (1979, 1980) for bridges in supercritical flows, or Qi *et al.* (2016) for Chinese rivers. The proposed model was previously validated for several flow conditions by Link *et al.* (2017, 2020), and the software ScourApp was recently published as part of a sensitivity analysis of the model parameters by Pizarro *et al.* (2022). As the computation of scour under clear water and live bed conditions is a difficult task, more field and laboratory evidence is needed for validation and verification of the model. However, the proposed method represents a significant improvement in the calculation of design scour, as it links it with occurrence probabilities.

The resulting time-dependent scour presented important variations during the study period. In some cases scour maxima were similar, while in other cases they exhibited maxima with notably different magnitudes. Series of extreme scour depths were computed with the annual maxima (AMAX) and partial duration series considering peaks over a threshold (POT). According to the efficiency values, POT series exhibited smaller variances of local scour depth corresponding to a return period

of T years than AMAX series, and thus POT was preferred for frequency analysis. Similarly to the flood frequency analysis, the use of each type of series for scour analysis presents advantages and disadvantages, as analysed by Zadeh *et al.* (2019).

Extreme maximum scour depths followed a Cauchy distribution, which has been previously used in many applications, such as mechanical and electrical theory, physical anthropology, measurement problems, and risk and financial analysis (Alzaatreh *et al.* 2016). It is different to other distributions commonly used for frequency analysis of extreme values, because it does not have finite moments of order greater than one. It is recognized as a heavy-tailed distribution. The Cauchy distribution was the only distribution able to compute realistic scour depths for high return periods, providing for the first time scour estimations associated with exceedance probabilities obtained from frequency analysis of extreme values.

The proposed methodology for the estimation of local scour depth at piers can be easily applied for other scour processes involved in bridge design, such as the general scour, contraction scour, and abutment scour. The new design philosophy involved considers scour as a stochastic process, and design scour is determined for a given return period. In this way, bridge design can be associated with probability of occurrence, and with risk. At the same time, the method can be applied to inform monitoring and maintenance, improving bridges' safety.

5 Conclusions

A method that computes the design local scour depth based on its probability of occurrence was proposed, introducing a probabilistic approach in bridge design for enhanced infrastructure risk management. The time evolution of local scour depth at bridge piers was computed considering refilling of the scour hole due to sediment deposition during flood recessions, and a proper frequency analysis of extreme maximum scour depth series was performed.

POT series were better suited than AMAX series of maximum scour depths for frequency analysis, and extreme scour depths at bridge piers followed a Cauchy distribution. Scour depths with a 100-year return period resulted in 22 to 202% of the equilibrium scour depth currently used in design.

Additional research is needed to provide more experimental and field evidence for further model validation. In this

Table 10. Dimensional and dimensionless local scour depth for different return periods.

Bridge	T 25 (years)		T 50 (years)		T 100 (years)		T 200 (years)	
	$R = 90\%$		$R = 70\%$		$R = 50\%$		$R = 26\%$	
	Z_s (m)	Z^*	Z_s (m)	Z^*	Z_s (m)	Z^*	Z_s (m)	Z^*
Ñuble	1.63	0.0261	2.41	0.0386	3.98	0.0637	7.11	0.1138
Biobío	0.50	0.0103	0.60	0.0123	0.79	0.0162	1.17	0.0240
Renaico	3.34	0.0079	5.56	0.0132	9.98	0.0237	18.82	0.0448
Donguil	1.78	0.0002	2.09	0.0003	2.77	0.0004	3.99	0.0005
Ciruelos	5.47	0.0130	6.53	0.0156	8.67	0.0207	12.93	0.0308
Leficahue	1.36	0.0038	1.53	0.0043	1.86	0.0053	2.53	0.0072
Río Bueno	4.28	0.0138	5.98	0.0193	9.37	0.0303	16.14	0.0522
Rahue	1.99	0.0158	2.42	0.0192	3.28	0.0261	5.01	0.0397
Forrahue	0.94	0.0006	1.10	0.0007	1.42	0.0008	2.08	0.0012
Cancura	0.40	0.0168	0.57	0.0243	0.92	0.0392	1.62	0.0689

context, the field measurement of scour during floods is especially challenging.

Acknowledgements

The authors thank the Chilean Empresa de los Ferrocarriles del Estado (EFE) for providing the basic data of the railway study bridges. This research was funded by FONDECYT 1221341.

Disclosure statement

No potential conflict of interest was reported by the authors.

ORCID

Pedro Arriagada  <http://orcid.org/0000-0001-6380-8769>

Oscar Link  <http://orcid.org/0000-0002-2188-6504>

References

- Alzaatreh, A., et al., 2016. The generalized Cauchy family of distributions with applications. *Journal of Statistical Distributions and Applications*, 3 (1), 12. doi:10.1186/s40488-016-0050-3
- American Standard for Testing Materials, 2017. *Standard test methods for particle-size distribution (Gradation) of soils using sieve analysis*. Standard No. D6913/D6913M. West Conshohocken: ASTM.
- American Standard for Testing Materials, 2018. *Standard practice for reducing samples of aggregate to testing size*. Standard No. C702/C702M. West Conshohocken: ASTM.
- American Standard for Testing Materials, 2019. *Standard practice for sampling aggregates*. Standard No. D75/D75M. West Conshohocken: ASTM.
- Arneson, L.A., et al., 2012. *Evaluating scour at bridges*. Hydraulic engineering circular No. 18. 5th ed. FHWA-HIF-12-003. Washington, DC, USA: US DOT.
- Arriagada, P., Karelovic, B., and Link, O., 2021. Automatic gap-filling of daily streamflow time series in data-scarce regions using a machine learning algorithm. *Journal of Hydrology*, 598 (2021), 126454. doi:10.1016/j.jhydrol.2021.126454
- Ben Aissia, M.A., Chebana, F., and Ouarda, T.B.M.J., 2017. Multivariate missing data in hydrology – review and applications. *Advances in Water Resources*, 110, 299–309. doi:10.1016/j.advwatres.2017.10.002
- Bolduc, L.C., Gardoni, P., and Briaud, J., 2008. Probability of exceedance estimates for scour depth around bridge piers. *Journal of Geotechnical and Geoenvironmental Engineering*, 134 (2), 175–184. doi:10.1061/(ASCE)1090-0241(2008)134:2(175)
- Borghesi, M.S., Kabiri-Samani, A., and Banihashem, S.A., 2012. Influence of unsteady flow hydrograph shape on local scouring around bridge pier. *Proceedings of the Institution of Civil Engineers-Water Management*, 165 (9), 473–480. doi:10.1680/wama.11.00020
- Breiman, L., 2001. Random forests. *Machine Learning*, 45 (1), 5–32. doi:10.1023/A:1010933404324.
- Breusers, H.N.C., Nicollet, G., and Shen, H.W., 1977. Local scour around cylindrical piers. *Journal of Hydraulic*, 15 (3), 211–252. doi:10.1080/00221687709499645
- Briaud, J.-L., et al., 2004. The SRICOSEFA computer program for bridge scour. *Invited Lecture. Proceedings of the Second International Conference on Scour and Erosion*. Singapore: Singapore (World Scientific Publishing Company).
- Briaud, J.L., et al., 2007. Probability of scour depth exceedance owing to hydrologic uncertainty. *Georisk*, 1 (2), 77–88.
- Chilean Ministry of Public Works (MOP), 2000. *Highways design manual (In Spanish)*. Santiago, Chile: Dirección de Vialidad. Ministerio de Obras Públicas.
- Chilean National Water Agency (DGA), 2021. *Streamflow gauges (SFG)*. Available from: <https://dga.mop.gob.cl/servicioshidrometeorologicos/Paginas/default.aspx> [Accessed Mar 2020].
- Chilean Railway Company (EFE), 2020. *Diagnosis of infrastructure of bridges and embankments of the EFE railway network*. Internal Report (in Spanish).
- Chow, V.T., 1994. *Open-Channel hydraulics*. 978-1932846188. New York: Mc Graw Hill.
- Contreras-Jara, M., et al., 2021. Estimation of exceedance probability of scour on bridges using reliability principles. *Journal of Hydrologic Engineering*, 26 (8), 04021029. doi:10.1061/(ASCE)HE.1943-5584.0002109
- Cook, W., Barr, P.J., and Halling, M.W., 2015. Bridge failure rate. *Journal of Performance of Constructed Facilities*, 29 (3), 04014080. doi:10.1061/(ASCE)CF.1943-5509.0000571
- Cunnane, C., 1973. A particular comparison of annual maxima and partial duration series methods of flood frequency prediction. *Journal of Hydrology*, 18 (3–4), 257–271. doi:10.1016/0022-1694(73)90051-6
- Dargahi, B., 1990. Controlling mechanism of local scouring. *Journal of Hydraulic Engineering*, 116 (10), 1197–1214. doi:10.1061/(ASCE)0733-9429(1990)116:10(1197)
- Dembélé, M., et al., 2019. Gap-filling of daily streamflow time series using direct sampling in various hydroclimatic settings. *Journal of Hydrology*, 569, 573–586. doi:10.1016/j.jhydrol.2018.11.076
- Dey, S., 1999. Time-variation of scour in the vicinity of circular piers. *Proceedings of the Institution of Civil Engineers - Water, Maritime and Energy*, 136 (2), 67–75. doi:10.1680/iwtme.1999.31422
- Flores-Vidriales, D., Gómez, R., and Tolentino, D., 2022. Stochastic assessment of Scour Hazard. *Water*, 14 (3), 273. doi:10.3390/w14030273
- German Association for Water, Wastewater and Waste (DWA), 2020. *Merkblatt DWA-M 529: auskolkungen an pfahlartigen Bauwerksgründungen*. Hennef, Germany: DWA.
- Gyau-Boakye, P. and Schultz, G.A., 1994. Filling gaps in runoff time series in West Africa. *Hydrological Sciences Journal*, 39 (6), 621–636. doi:10.1080/02626669409492784.
- Harvey, C.L., Dixon, H., and Hannaford, J., 2012. An appraisal of the performance of data-infilling methods for application to daily mean river flow records in the UK. *Hydrology Research*, 43 (5), 618–636. doi:10.2166/nh.2012.110.
- Hong, J.H., et al., 2016. A new practical method to simulate flood-induced bridge pier scour-A case study of Mingchu bridge piers on the Cho-Shui River. *Water (Switzerland)*, 8 (6), 238.
- Jain, S.C. and Fischer, E.E. (1979). Scour around circular bridge piers at high Froude numbers (No. FHWA-RD-79-104 Final Rpt.)
- Jain, S.C. and Fischer, E.E., 1980. Scour around bridge piers at high flow velocities. *Journal of the Hydraulics Division*, 106 (11), 1827–1842. doi:10.1061/JYCEAJ.0005560
- Johnson, P.A. and Ayyub, B.M., 1992. Assessing time variant bridge reliability due to pier scour. *Journal of Hydraulic Engineering*, 118 (6), 887–903. doi:10.1061/(ASCE)0733-9429(1992)118:6(887)
- Johnson, P.A. and Dock, D.A., 1998. Probabilistic bridge scour estimates. *Journal of Hydraulic Engineering*, 124 (7), 750–754. doi:10.1061/(ASCE)0733-9429(1998)124:7(750)
- Khalid, M., Muzzammil, M., and Alam, J., 2019. A reliability-based assessment of live bed scour at bridge piers. *ISH Journal of Hydraulic Engineering* 27 (S1), 105–112. <https://doi.org/10.1080/09715010.2019.1584543>
- Kim, M., et al., 2015. Comparative studies of different imputation methods for recovering streamflow observation. *Water (Switzerland)*, 7, 6847–6860. doi:10.3390/w7126663
- Kobierska, F., Engeland, K., and Thorarinsdottir, T.L., 2017. Evaluation of design flood estimates – a case study for Norway. *Hydrology Research*, 49 (2), 450–465. doi:10.2166/nh.2017.068
- Lang, M., Ouarda, T.B.M.J., and Bobée, B., 1999. Towards operational guidelines for over-threshold modelling. *Journal of Hydrology*, 225 (3–4), 103–117. doi:10.1016/S0022-1694(99)00167-5
- Lee, W.-L., Lu, C.-W., and Huang, C.-K., 2021. A study on interaction between overfall types and scour at bridge piers with a moving-bed experiment. *Water*, 13 (2), 152. doi:10.3390/w13020152
- Li, H., et al., 2018. What large sample size is sufficient for hydrologic frequency analysis?—A rational argument for a 30-year hydrologic

- sample size in water resources management. *Water*, 10 (4), 430. doi:10.3390/w10040430
- Link, O., et al., 2017. A model of bridge pier scour during flood waves. *Journal of Hydraulic Research*, 55 (3), 310–323. doi:10.1080/00221686.2016.1252802
- Link, O., et al., 2020. Local scour and sediment deposition at bridge piers during floods. *Journal of Hydraulic Engineering*, 146 (3), 04020003. doi:10.1061/(ASCE)HY.1943-7900.0001696
- López, G., et al., 2014. Estimating final scour depth under clear-water flood waves. *Journal of Hydraulic Engineering*, 140 (3), 328–332. doi:10.1061/(ASCE)HY.1943-7900.0000804
- Lu, J.-Y., et al., 2008. Field measurements and simulation of bridge scour depth variations during floods. *Journal of Hydraulic Engineering*, 134 (6), 810–821. doi:10.1061/(ASCE)0733-9429(2008)134:6(810)
- Manfreda, S., Link, O., and Pizarro, A., 2018. A theoretically derived probability distribution of scour. *Water (Switzerland)*, 12, 374. doi:10.3390/w12020374
- Melville, B.W. and Coleman, S.E., 2000. *Bridge scour*. 1887201181. Littleton, CO, USA: Water Resources Publications, LLC.
- Meyer-Peter, E. and Müller, R., 1948. Formulas for bed-load transport. In Vol. A2 of Proc., 2nd IAHR Congress, 1–26. Delft, Netherlands: International Association for Hydro-Environment Engineering and Research.
- Muñoz, P., et al., 2018. Flash-flood forecasting in an andean mountain catchment-development of a step-wise methodology based on the random forest algorithm. *Water (Switzerland)*. 10. doi:10.3390/w10111519
- Mwale, F.D., Adeloje, A.J., and Rustum, R., 2012. Infilling of missing rainfall and streamflow data in the Shire River basin, Malawi - A self organizing map approach. *Physics and Chemistry of the Earth*, , Parts A/B/C 50-52, 34–43. doi:10.1016/j.pce.2012.09.006
- Pizarro, A., et al., 2017. Dimensionless effective flow work for estimation of pier scour caused by flood waves. *Journal of Hydraulic Engineering*, 143 (7), 06017006. doi:10.1061/(ASCE)HY.1943-7900.0001295
- Pizarro, A., Ettmer, B., and Link, O., 2022. Relative importance of parameters controlling scour at bridge piers using the new toolbox ScourApp. *Computers & Geosciences*, 163, 105117. doi:10.1016/j.cageo.2022.105117
- Pizarro, A., Manfreda, S., and Tubaldi, E., 2020. The science behind scour at bridge foundations: a review. *Water*, 12 (2), 374. doi:10.3390/w12020374
- Qi, M., Li, J., and Chen, Q., 2016. Comparison of existing equations for local scour at bridge piers: parameter influence and validation. *Natural Hazards*, 82 (3), 2089–2105. doi:10.1007/s11069-016-2287-z
- Raudkivi, A.J., 1986. Functional trends of scour at bridge pier. *Journal of Hydraulic Engineering*, 112 (1), 1–13. doi:10.1061/(ASCE)0733-9429(1986)112:1(1)
- Shahriar, A.R., et al., 2021. Quantifying probability of deceedance estimates of clear water local scour around bridge piers. *Journal of Hydrology*, 597, 126177. doi:10.1016/j.jhydrol.2021.126177
- Sheppard, D.M., Melville, B., and Demir, H., 2014. Evaluation of existing equations for local scour at bridge piers. *Journal of Hydraulic Engineering*, 140 (1), 14–23. doi:10.1061/(ASCE)HY.1943-7900.0000800
- Sidibe, M., et al., 2018. Trend and variability in a new, reconstructed streamflow dataset for West and Central Africa, and climatic interactions, 1950–2005. *Journal of Hydrology*, 561, 478–493. doi:10.1016/j.jhydrol.2018.04.024
- Stedinger, J.R., Vogel, R.M., Foufoula-Georgiou, E., 1993. Frequency analysis of extreme events, and D.R. Maidment, ed. *Handbook of hydrology*. New York: McGraw-Hill, 18.1–18.66.
- Stekhoven, D.J. and Bühlmann, P., 2012. Missforest-Non-parametric missing value imputation for mixed-type data. *Bioinformatics*, 28 (1), 112–118. doi:10.1093/bioinformatics/btr597.
- Tang, F. and Ishwaran, H., 2017. Random forest missing data algorithms. *Statistical Analysis and Data Mining: The ASA Data Science Journal*, 10 (6), 363–377. doi:10.1002/sam.11348.
- Tubaldi, E., et al., 2017. A framework for probabilistic assessment of clear-water scour around bridge piers. *Structural Safety*, 69, 11–22. doi:10.1016/j.strusafe.2017.07.001
- Vega-García, C., Decuyper, M., and Alcázar, J., 2019. Applying cascade-correlation neural networks to in-fill gaps in mediterranean daily flow data series. *Water*, 11 (8), 1691. doi:10.3390/w11081691.
- Wardhana, K. and Hadipriono, F.C., 2003. Study of recent building failures in the United States. *Journal of Performance of Constructed Facilities*, 17 (3), 151–158. doi:10.1061/(ASCE)0887-3828(2003)17:3(151)
- Yan, L., et al., 2021. Design flood estimation with varying record lengths in Norway under stationarity and nonstationarity scenarios. *Hydrology Research*, 52 (6), 1596–1614. doi:10.2166/nh.2021.026
- Zadeh, K.F., et al., 2019. Impact of measurement error and uncertainty quantification. *Environmental Modelling and Software*, 118 (3), 35–47. doi:10.1016/j.envsoft.2019.03.022
- Zanke, U., 1977. *Neuer Ansatz zur Berechnung des Transportbeginns von Sedimenten unter Stromungseinfluss in German*. Hannover, Germany: Mitteilungen des Franzius-Institut, Technical Univ. Hannover.
- Zanke, U., 1982. Kolke am Pfeiler in richtungskonstanter Strömung und unter Welleneinfluß. Mitteilungen des Franzius-Instituts, Technical Universität. Hannover, 54, 381–416.